Theor Chem Acc (2003) 109:220–228
DOI 10.1007/s00214-002-0401-7

Theoretical
Chemistry Accounts

Regular article

Molecular dynamics study of the tautomeric equilibrium in the 4-nitro- and 2,4,6-trichloro derivatives of 2-(*N*,*N*-dialkyloaminomethyl)phenol

A. Fedorowicz[1], **A. Koll**[1], **J. Mavri**[2]

[1] Faculty of Chemistry, University of Wroclaw, F. Joliot-Curie 14, 50-383 Wroclaw, Poland
[2] National Institute of Chemistry, Hajdrihova 19, Ljubljana 1000, Slovenia

Received: 26 April 2002 / Accepted: 9 September 2002 / Published online: 31 March 2003

Abstract. Molecular dynamics thermodynamic integration (MDTI) method and quantum chemical calculations at the density functional theory B3LYP 6-31 + (d,p) level, which included the Tomasi model of the solvent reaction field, were applied to study the tautomeric equilibrium of Mannich base in methanol solution. The values obtained for the free-energy difference are in good agreement with experimental data. However, the results from quantum mechanical calculations were not as good as the results of MDTI simulations owing to inappropriate treatment of intermolecular hydrogen bonds between the solute molecule and the first shell of solvent molecules in the Tomasi model of the solvent reaction field. The radial distribution functions between solute atoms and solvent atoms confirmed the formation of hydrogen bonds between the solute molecule and surrounding methanol molecules and indicated that the zwitterionic form is associated more with an organized solvent structure at the level of the first solvation shell than is the molecular form.

Keywords: Mannich base – Tautomerism – Molecular dynamics – Thermodynamic integration – Solvent effect

Introduction

The knowledge of the molecular properties of tautomeric equilibrium and especially conditions in which the key process of the intramolecular proton transfer occurs is very important in understanding properties of biological systems and other important materials. The study of the nature of these processes is complicated by the fact that they happen mostly in a strongly fluctuating environment, either in the solution or inside macromolecular systems, like peptides.

The products of condensation of the formaldehyde, secondary amine and phenol derivative appear to be a model system for studying the intramolecular proton-transfer process [1, 2, 3, 4], which is a key element in understanding the tautomeric phenomena. These chemical compounds are called Mannich bases after the name of the reaction by which they are synthesized [5].

It has been experimentally observed that the properties of a system with an intramolecular hydrogen bond depend both on the external and on the internal conditions [6], where the internal conditions are related to the molecular properties of the chemical compound itself, like the energy difference between two forms in the gas phase. The external conditions thus mean all the factors that change the molecular properties upon transfer to a given system. The internal conditions, like the energy difference between different forms, can be estimated by means of quantum mechanical calculations. An experimental study has shown for Mannich bases, where the tautomeric equilibrium was observed, that the zwitterionic form has a lower energy and the process of temperature decreasing increases the ratio for this form [7].

The intramolecular proton-transfer process (Fig. 1) is associated with a dynamical reorganization of the solvent molecules. Although this reorganization is much slower than the proton-transfer process itself, experimental studies have shown that a decrease in the temperature of the solution of the Mannich base below the freezing point inhibits a further shift in the tautomeric equilibrium towards the zwitterionic form [8]. Moreover, it has been found that the proton-transfer process is associated with a strong negative entropy change of the order of −5 to −15 cal mol^{-1} K^{-1}, and it has been sug-

Contribution to the 8th Electronic Computational Chemistry Conference, 2002

Electronic Supplementary Material to this paper (full text of the lecture in html as given at the ECCC8 conference) can be obtained by using the SpringerLink server located at http://dx.doi.org/10.1007/s00214-002-0401-7.

Correspondence to: A. Fedorowicz
Present address: National Institute of Occupational Safety and Health, 1095 Willowdale Road, Morgantown, WV 26505, USA
e-mail: ajf4@cdc.gov

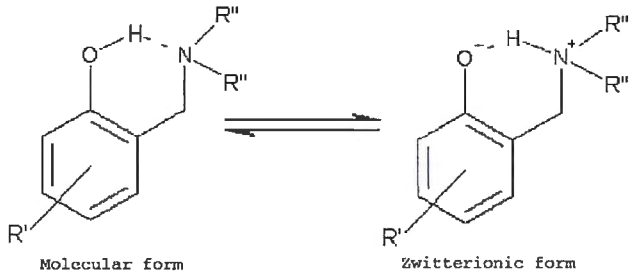

Fig. 1. Tautomeric equilibrium in the Mannich base

gested that this process is probably associated with changes in solvent structure, thus providing a source for such entropy change.

In this report, we present the results of the computer simulations for two selected sets of Mannich bases, namely the 4-nitro and 3,4,6-trichloro derivatives of 2-(*N*,*N*-dialkyloaminomethyl)phenol [7]. For the study of the internal conditions associated with the proton-transfer process, quantum mechanical methods were applied, which provided parameters that were subsequently used to adjust the Gromos96 force field, which was later applied to study the external conditions by means of molecular dynamics (MD) simulations. The main aim of these computational studies was to estimate the free-energy difference associated with the tautomeric equilibrium in the Mannich bases. Three methods of estimation of the free-energy difference were applied and compared: the quantum mechanical Tomasi model of the solvent reaction field (PCM), and two techniques of the thermodynamic integration method, slow growth and the multi-configurational thermodynamic integration approach based on the Gauss–Legendre quadrature [8]. Because the simulations presented were focused on the estimation of the free-energy difference between two tautomeric forms (molecular and zwitterionic), which does not depend on the reaction pathway, this report does not address the question about the reaction pathway, energy barriers and proton tunneling. During the MD thermodynamic integration (MDTI) simulations, which were used to simulate the proton transfer, a commonly used linear approach was applied that cannot give information about the reaction pathway or proton tunneling:

$$H(\lambda) = \lambda H(\mathrm{B}) + (1 - \lambda)H(\mathrm{A}) \ ,$$

where $H(\lambda)$ is the actual Hamiltonian that describes the current state, $H(\mathrm{A})$ is the Hamiltonian of the initial form, $H(\mathrm{B})$ is the Hamiltonian of the final form, and λ is the coupling parameter which is steadily changed during MDTI simulation from the initial value of 0 corresponding to the initial state A, to the value of 1 corresponding to the final state B.

The adjustment of the force field was based on the application of the atomic charges, obtained according to the Merz–Singh–Kollman procedure, which fits them to the electrostatic field with the presence of the surrounding solvent modeled by the solvent reaction field. Moreover, the selected geometry parameters, like bond lengths and bond angles, were adjusted to the values obtained from the quantum mechanical calculations.

Computational

Geometry optimizations of the zwitterionic and the neutral forms of the Mannich bases were carried out in vacuo at the Becke3LYP 6-31+G(d,p) level. The valence basis set applied, augmented with the polarization functions and diffuse functions on heavy atoms, is flexible enough to faithfully reproduce the energetics of the proton-transfer process. The density functional theory (DFT) scheme was used with the exchange functionals proposed by Becke [10], and the correlation functional proposed by Lee, Yang and Parr [11]. The quantum chemical calculations were carried out using the GAUSSIAN98 suite of programs [12].

During geometry optimization of the zwitterionic form structures, the proton associated with the hydrogen bond moved in all cases into the neutral form position. For this reason, the N–H distance was frozen at 1.05 Å for all the zwitterionic forms. The fact that the N–H distance for the zwitterionic form was not fully optimized leads only to a relatively small error in the calculations because it concerns mostly the high frequency ν (N–H) vibrations and thus its influence should not be too great in systems. Additionally, one can mention that all the frequency calculations did not show any imaginary values for the zwitterionic forms, suggesting that the calculations were performed for the stationary data.

Subsequently, single-point quantum chemical calculations were performed with application of the solvent reaction field model proposed by Miertus and Tomasi [13] and Tomasi and Persico [14] at the same DFT level, for both forms of the Mannich bases studied in methanol solution. These calculations provided sets of atomic charges for both forms of the solute molecules that take into account the presence of the solvent as a constant dielectric continuum. Atomic charges were calculated according to the Merz–Singh–Kollman scheme [15, 16], which reproduces the electrostatic potential around the molecule. This scheme provides an electrostatic model that gives rise to a more realistic description of the influence of the solvent environment on the distribution of atomic charges for each Mannich base, compared to the application of the atomic charges derived from calculation in the gas phase, hence leading to a much better description of the electrostatic interaction of the solute molecule with solvent during further MD simulations.

Moreover, application of the Tomasi model of the solvent reaction field provided values of the free-energy difference between the two tautomeric forms of the Mannich bases studied in methanol solution; however, this approach has its own limitations and does not take into account any explicit interaction between solute and solvent molecules, especially the formation of intramolecular hydrogen bonds between solute and solvent molecules.

During the next stage, MD simulations in the gas phase and in solution were conducted independently for each Mannich base using the GROMOS96 suite of programs [17]. During the MD simulations, the modified GROMOS96 force field was applied. The parameterization of the force field consisted of application of the atomic charges and selected geometry parameters obtained from quantum chemical calculations. The force constants and van der Waals parameters were not adjusted. For the simulations of systems with solvent molecules the standard GROMOS96 description of methanol was applied.

All the MD simulations in vacuo were performed with a timestep of 1 fs. The temperature of 298.15 K was maintained by the Berendsen model with a relaxation time of 0.2 ps [18]. The structures corresponding to the molecular form were equilibrated in 1,000-ps simulations in vacuo. These simulations provided equilibrated structures in the gas phase of the molecular form. Subsequently, the series of 1,000-ps MDTI simulations, with application of the slow growth technique, were carried out with gradual changes of the parameter λ from 0 to 1 and back from 1 to 0. This means that the

systems underwent linear evolution from the molecular form ($\lambda = 0$) to the zwitterionic form ($\lambda = 1$) and then back from zwitterionic to molecular form. The values of the potential-energy derivative as a function of λ were collected every 100 fs. These simulations provided the free-energy differences in the gas phase, $\Delta A_{\text{in vacuo}}$, between the zwitterionic form and the molecular form of the given Mannich base by using the slow growth method:

$$\Delta A = \sum_i \left(\frac{\partial U}{\partial \lambda}\right)_i \Delta\lambda \ .$$

The next set of calculations consisted of ten MD simulations at constant values of the λ. These values correspond to the values of abscissas, which are necessary to apply the Gauss–Legendre quadrature to integrate the derivative of the potential energy as a function of λ. During these simulations the values of λ were kept constant. After 200-ps equilibrating simulations, additional 200-ps simulations were conducted for which the values of $\delta U/\delta\lambda$ were collected every 100 fs. Subsequently, the mean values of $\delta U/\delta\lambda$ were calculated for each value of λ and then integrated by the Gauss–Legendre quadrature, which gave rise to the free-energy differences in vacuo, $\Delta A_{\text{in vacuo}}$ (gl), for each Mannich base considered:

$$\Delta A = \int_0^1 \left\langle \frac{\partial U}{\partial \lambda} \right\rangle_\lambda \mathrm{d}\lambda \ .$$

The MD simulations in solution were conducted in the microcanonical NVT ensemble with a timestep of 1 fs. The Berendsen model of temperature control was applied with a relaxation time of 0.2 ps and with a cutoff value for nonbonded interactions of 12.0 Å. The study of the given Mannich base in the solution started from building a box containing one solute molecule and more than 200 methanol molecules. This number of solvent molecules with one solute molecule reproduces fairly well the experimental density of the pure solvent for the given box size.

The MD calculations started from simulations where the temperature was raised stepwise from 10 to 50 K and 100 to 298.15 K each 50 ps in 1-fs steps. After equilibration, systems with molecular form were applied as initial structures for MDTI simulations with application of the slow growth technique. During these simulations, each 200 ps, the molecular form ($\lambda = 0$) was transformed into the zwitterionic form ($\lambda = 1$) and then back to the molecular form. The values of the differential $\delta U/\delta\lambda$ were collected every 100 fs and then integrated numerically to produce the free-energy difference in solution, $\Delta A_{\text{in solution}}$ (sg).

Subsequent sets of calculations were performed for each system with ten different and constant values of λ, which corresponded to the values necessary to apply the Gauss–Legendre quadrature. During these simulations, the value of λ was kept constant. After 200-ps equilibrating calculations, additional 200-ps simulations were conducted and the values of $\delta U/\delta\lambda$ were collected every 100 fs. The mean values of $\delta U/\delta\lambda$ were calculated for each value of λ and were then integrated by the Gauss–Legendre quadrature, which gave rise to the free-energy difference in solution, $\Delta A_{\text{in solution}}$ (gl).

The total free-energy difference, ΔA, which describes tautomeric equilibrium in the Mannich bases, was calculated according to the formula

$$\Delta A = \Delta A_{\text{in solution}} - \Delta A_{\text{in vacuo}} + \Delta E_{\text{QC}} \ ,$$

where ΔE_{QC} is the energy difference between the zwitterionic form and the molecular form from DFT calculations, $\Delta A_{\text{in solution}}$ is the free-energy difference obtained from MDTI simulation in solution and $\Delta A_{\text{in vacuo}}$ is the free-energy difference obtained from MDTI simulation in vacuo. In our previous report [3], where we studied the tautomeric equilibrium in 2-(*N*,*N*-dimethylaminomethyl)-3,4,6-trichlorophenol, we also included the zero-point-energy difference term (ΔZPE). However, it had a low value of 0.3 kcal mol^{-1}, which was 5 times lower than the error of the MDTI simulations. Therefore, in the present study, after comparing values of the computed ΔZPE ranging from 0.1 to 0.3 kcal mol^{-1}, in most cases this correction was again much smaller than the error of the MDTI simulations, and thus we decided to omit this factor because it had a marginal influence on the computed value of the free-energy difference compared to MDTI errors. However, we acknowledge that this term can be significant in studies of intramolecular proton-transfer processes [20] and has to be checked every time.

The MD method is not the most efficient tool for estimating the energy difference between two given forms, since the force fields are still in the development phase and it is known that they provide correct results mostly for the compounds that are used to derive such force fields. Thus, in our approach we decided to extract the part in the total free-energy difference that describes the proton transfer itself in vacuo ($\Delta A_{\text{in vacuo}}$) and replace it by a more correct value from the quantum mechanical calculation (ΔE_{QC}). Therefore, our result represents a mixture of the quantum chemical calculations, which describe the "internal" conditions, and classical MD simulations, which describe the "external" conditions, namely solute–solvent, and solvent–solvent interactions.

During the last stage, single 200-ps MD simulations were performed for systems with the molecular form and for systems with the zwitterionic form, preceded by 200-ps equilibrating calculations. The systems with the zwitterionic form were maintained by keeping the value of λ at the constant value of 1, which corresponds to the Hamiltonian that describes this form. The coordinate trajectory was recorded every 100 fs. The radial distribution functions between selected solute atoms and solvent atoms were estimated and compared for differences between systems with the molecular form and systems with the zwitterionic form. Radial distribution functions were subsequently calculated using the following formula [19]:

$$g(r) = \frac{n(r)}{4\partial r^2 \tilde{n}} \ ,$$

where $n(r)$ is the number of atoms considered inside a layer between a distance of r to $r + \mathrm{d}r$ from a central atom, and the ρ is the density, which equals N/V, where N is the total number of atoms considered and V is the volume of the system. Values for $n(r)$ were taken from a histogram, which was normalized with respect to the number of steps [19].

Results

The results of the DFT calculations with application of the solvent reaction field and the MDTI simulations are collected and compared with experimental values in Table 1.

The computed values of the free-energy difference are in good agreement with the experimental data, and especially the approach based on the Gauss–Legendre quadrature resulted in the best agreement. The slightly worse results for the slow growth technique are related to the common fact that calculations based on the application of this approach often have a greater error owing to inefficient system equilibration for a given value of λ. The weaker performance of the solvent reaction field PCM method (ΔA_{PCM}) is probably related to an inadequate description by this approach of direct interactions between the solute molecule and solvent molecules and, especially, the formation of intermolecular hydrogen bonds.

The formation of hydrogen bonds between the solute molecule of Mannich base and surrounding methanol molecules was found during investigation of the radial distribution functions between the solute phenol oxygen

Table 1. The comparison between the experimental free-energy difference describing tautomeric equilibrium in Mannich bases and the results of molecular dynamics thermodynamic integration simulations and quantum chemical calculations using the solvent reaction field

Alkyl group	ΔE_{QC} (kcal mol^{-1})	ΔA_{PCM} (kcal mol^{-1})	ΔA_{sg} (kcal mol^{-1})	ΔA_{gl} (kcal mol^{-1})	ΔG_{exp} (kcal mol^{-1})	ΔS_{exp} (cal mol K)
2-(*N*,*N*-Dialkylaminomethyl)-3,4,6-trichlorophenols						
Methyl	12.64	−1.45	0.4±0.8	0.26	0.12	−8.80
Ethyl	11.73	1.65	0.3±0.6	0.04	0.06	−7.77
Propyl	1.48	2.54	0.6±0.1	0.26	0.13	−7.34
Butyl	8.68	−0.63	0.6±0.4	0.45	0.18	−7.06
2-(*N*,*N*-Dialkylaminomethyl)-4-nitrophenols						
Methyl	14.71	1.25	0.06±0.06	0.35	0.02	−7.56
Ethyl	9.42	1.13	1.1±0.2	0.47	0.48	−8.61
Propyl	1.35	2.58	1.0±1.2	0.21	0.57	−8.59
Butyl	8.11	0.26	0.2±0.8	0.40	0.11	−7.10

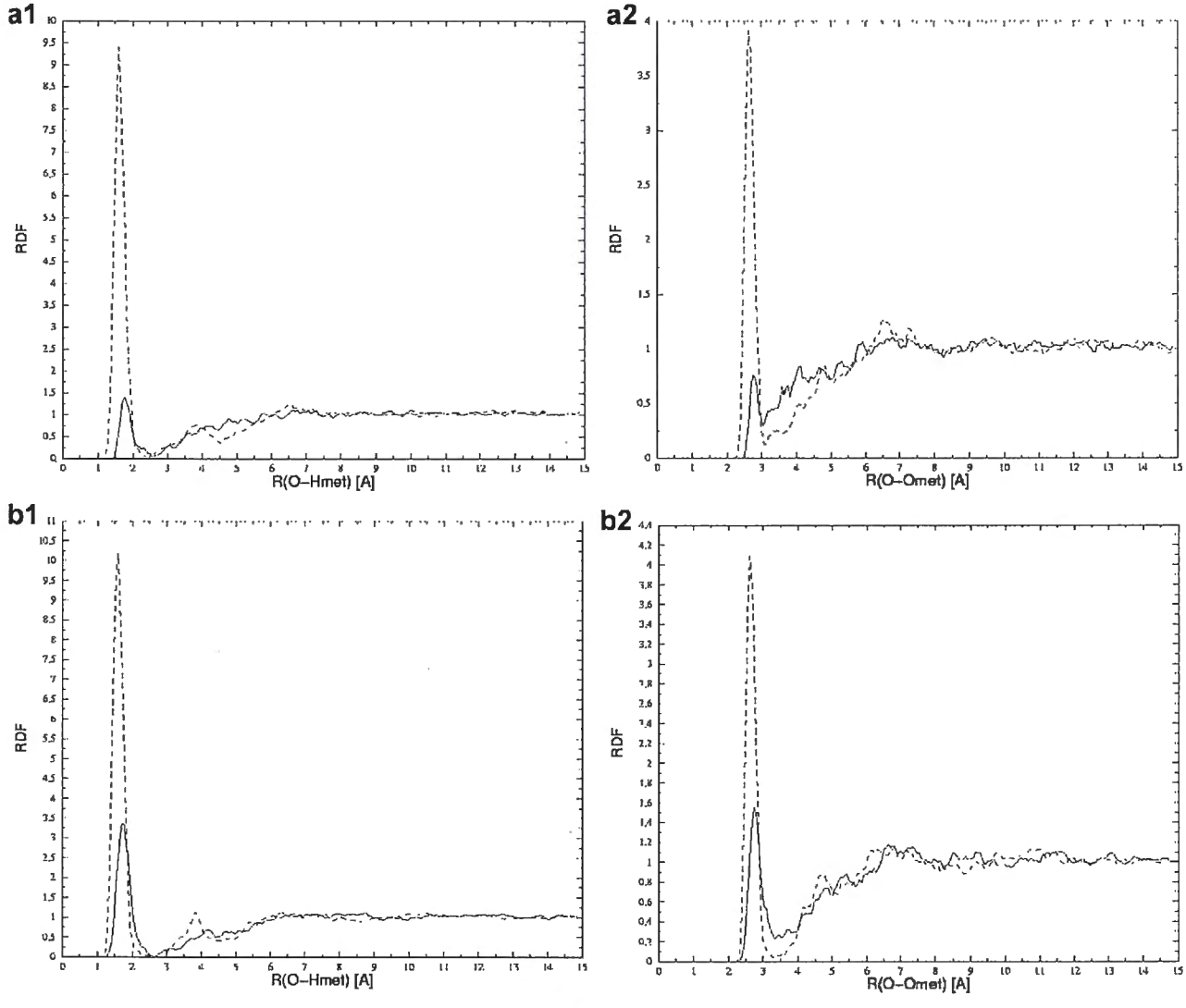

Fig. 2a–d. Radial distribution functions between the solute oxygen atom (O) and methanol (solvent) hydroxyl hydrogen (Hmet) and oxygen (Omet) atoms for 2-(*N*,*N*-dialkylaminomethyl)-3,4,6-trichlorophenols. The plots are ordered according to increase in the size of the alkyl groups attached to the amine nitrogen in the Mannich base: **a** methyl, **b** ethyl, **c** propyl, and **d** butyl. The *solid line* corresponds to the molecular form and the *dashed line* to the zwitterionic form

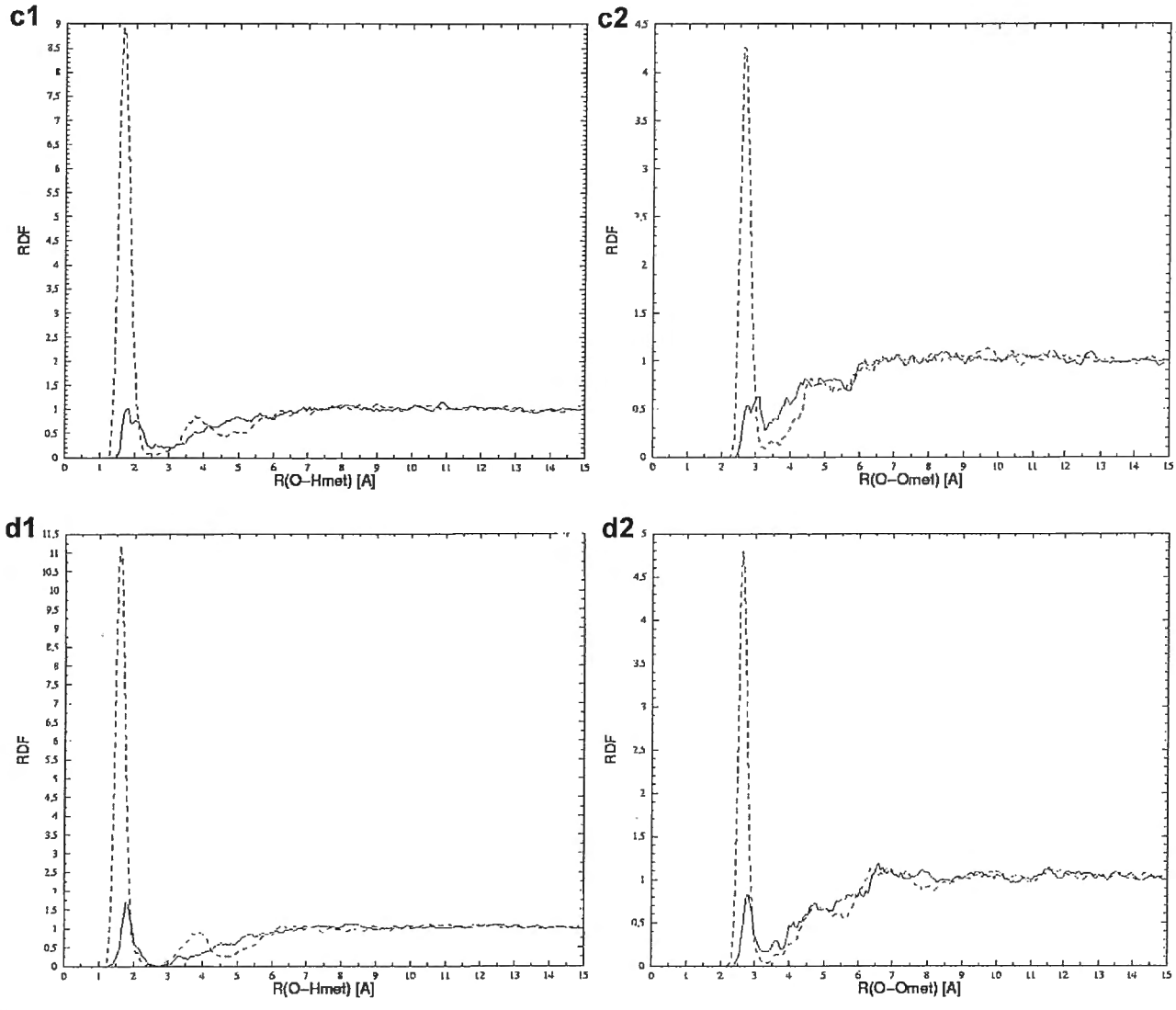

Fig. 2. (Contd.)

atom and solvent oxygen and hydroxyl hydrogen atoms. The comparisons between the radial distribution functions for the systems with the molecular forms and the radial distribution functions of the systems with the zwitterionic form are presented in the Figs. 2 and 3.

The radial distribution functions, presented in Figs. 2 and 3, show formation of hydrogen bonds between solute oxygen and solvent molecules. The peaks at 1.7 Å at the radial distribution function of O–Hmet correspond to systems with such bonds. The coordination numbers evaluated from those peaks are collected in Table 2 and indicate that the systems with the zwitterionic form have at least one solvent molecule more in the first shell than the systems with the molecular form. Therefore, the systems with the more polar zwitterionic form seem to be more "organized" in terms of the solvent structure, at least to a local extent. This phenomenon can be related to the experimental negative value of the entropy change, which suggests an increase in the organization of the solvent structure in the case of the systems with the zwitterionic form. It cannot be concluded that the solvent follows the intramolecular proton-transfer process since the time difference is too great between these two processes. However, one can say that the solvent constant fluctuations, which sometimes lead to the more organized systems, (at least to a local extent around the solute molecule) are more favored and may drive one form to another.

Another interesting feature, which was found from an analysis of the radial distribution functions, is the lack of hydrogen bonds between solute molecules and the solvent molecules either with participation of the hydrogen atom from the intramolecular hydrogen-bond bridge or with participation of the amine nitrogen atom (Fig. 4), for all systems studied.

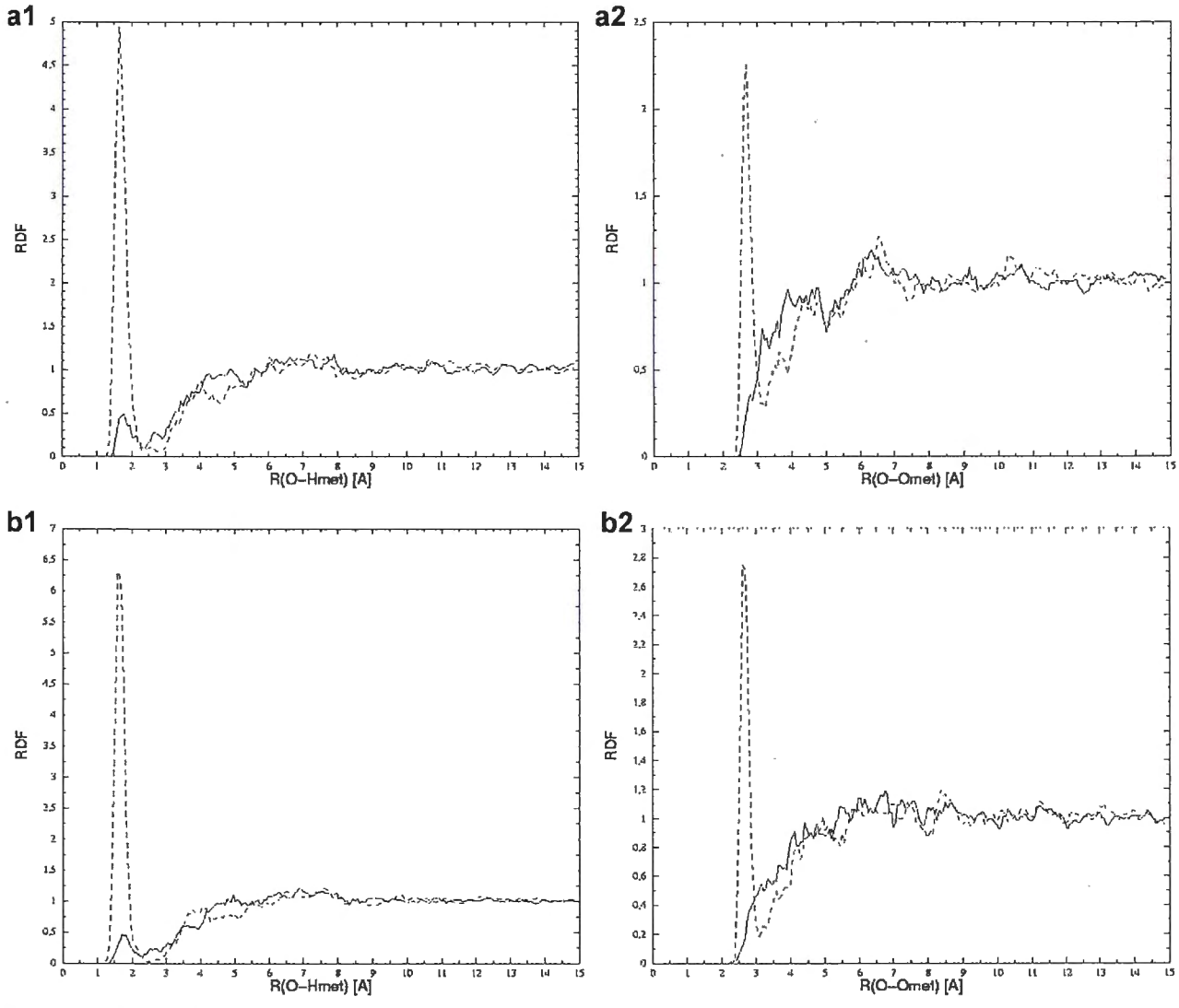

Fig. 3a–d. Radial distribution functions between the solute oxygen atom (O) and methanol (solvent) hydroxyl hydrogen (Hmet) and oxygen (Omet) atoms for 2-(*N*,*N*-dialkylaminomethyl)-4-nitrophenols. The plots are ordered according to increase in the size of the alkyl groups attached to the amine nitrogen in the Mannich base: **a** methyl, **b** ethyl, **c** propyl, and **d** butyl. The *solid line* corresponds to the molecular form and the *dashed line* to the zwitterionic form

Figure 4 shows two such radial distribution functions for 2-(*N*,*N*-dimethylaminomethyl)-3,4,6-trichlorophenol. Analogous radial distribution functions for other Mannich bases considered look similar to the plots presented here.

A comparison of the radial distribution functions between solvent atoms Omet–Hmet and Omet–Omet for 2-(*N*,*N*-dialkylaminomethyl)-3,4,6-trichlorophenols is presented in Fig. 5. Similar plots were obtained for the 2-(*N*,*N*-dialkylaminomethyl)-4-nitrophenols and were similar to plots already presented. The difference in the solvent structure between systems containing Mannich bases with increasing size of the alkyl group attached to the amine nitrogen atom is shown in Fig. 5. The greatest difference is for the systems with the propyl group either in the case of the nitro derivatives (not presented) or in the case of 3,4,6-trichloro derivatives. It seems that this alkyl group is associated with a much more distorted solvent structure than the other groups, even the bulky butyl group, which appears to behave almost like the smallest methyl group. One must mention that no effect of the proton transfer on these two radial distribution functions was observed in all eight Mannich bases, and therefore the observed increase of the solvent structure organization for the systems with the zwitterionic form must have only a local extent, with no implication for the total structure.

Discussion

The free-energy difference associated with the tautomeric equilibrium in the Mannich bases in methanol

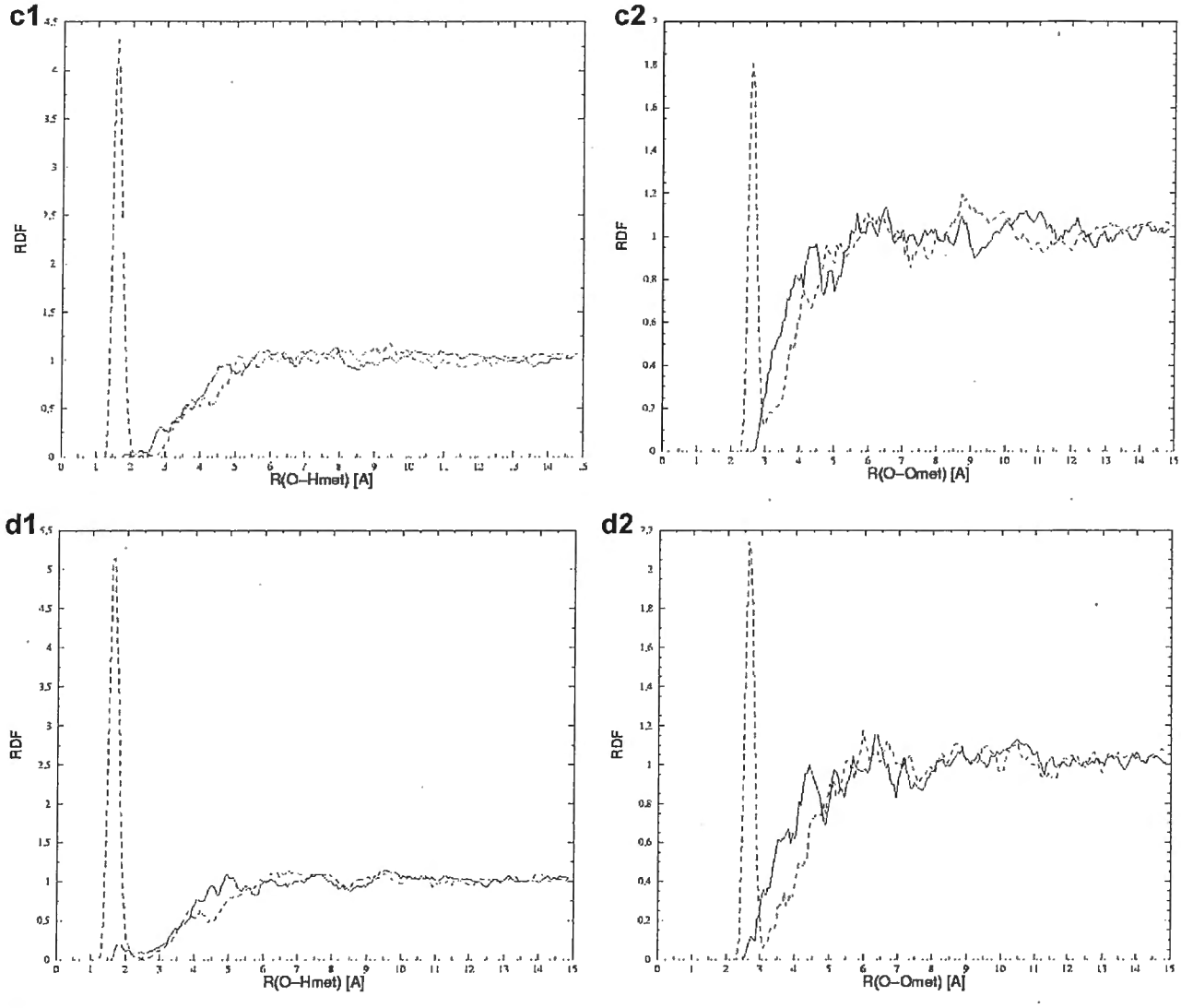

Fig. 3. Continued

solution was estimated by using the DFT method with the application of the solvent reaction field and a combination of quantum mechanical calculations with an all-atom representation of the solvent by MDTI simulations. In the latter case, thermal averaging was performed by MD and the free-energy difference was calculated using two techniques of the thermodynamic integration method. The computed free-energy values are in good agreement with the experimental results. The solvent reaction field gave the greatest difference, probably owing to an inappropriate description of the hydrogen bonds that can be formed between solute molecule and surrounding solvent molecules. The results based on the thermodynamic integration method with application of the Gauss–Legendre quadrature gave rise to excellent agreement with experiment, whereas the slow growth technique was slightly worse owing to a greater error related to the "flying" equilibration of the system.

Table 2. Coordination numbers for the first solvation shell calculated from the radial distribution function O–Hmet

Alkyl group	Molecular form	Zwitterionic form
2-(*N*,*N*-Dialkylaminomethyl)-3,4,6-trichlorophenols		
Methyl	0.34	1.65
Ethyl	0.91	1.78
Propyl	0.36	1.80
Butyl	0.44	1.92
2-(*N*,*N*-Dialkylaminomethyl)-4-nitrophenols		
Methyl	0.16	1.01
Ethyl	0.13	1.03
Propyl	0.00	1.63
Butyl	0.06	0.96

An analysis of the radial distribution functions revealed that the systems with the zwitterionic form are more favorable when the solvent fluctuating structure takes slightly more organized forms—which can be related to the experimental observation that lowering the

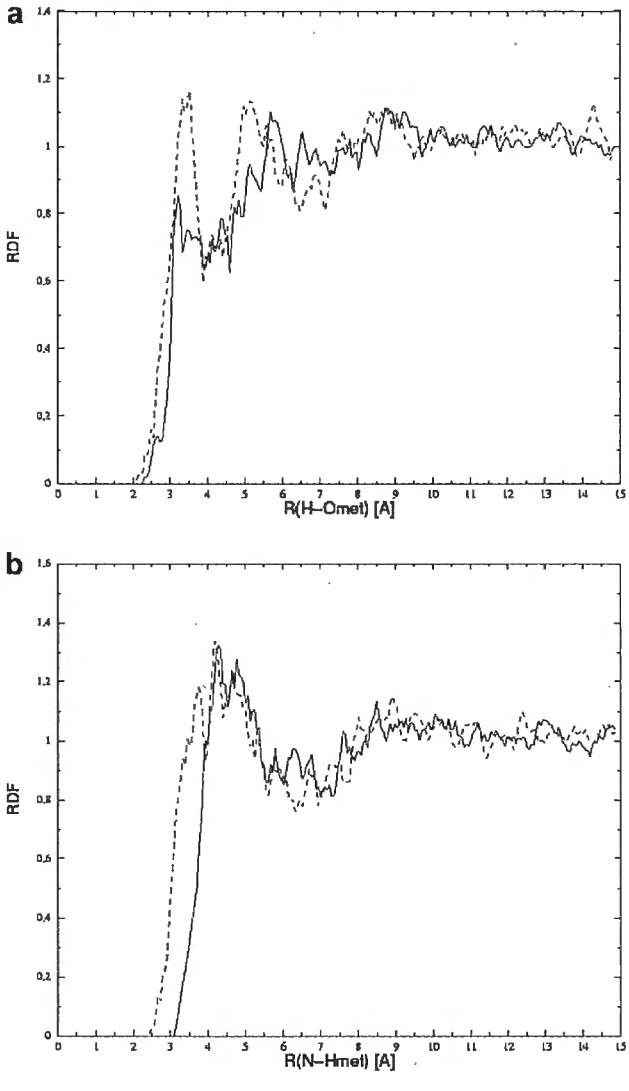

Fig. 4. Radial distribution functions **a** between the solute atom H from the OH group and methanol (solvent) oxygen (Omet) atoms, and **b** between the solute amine nitrogen atom N and solvent hydroxyl hydrogen (Hmet) atoms in the case of 2-(*N*,*N*-dimethylaminomethyl)-3,4,6-trichlorophenol. The *solid line* corresponds to the molecular form and the *dashed line* to the zwitterionic form

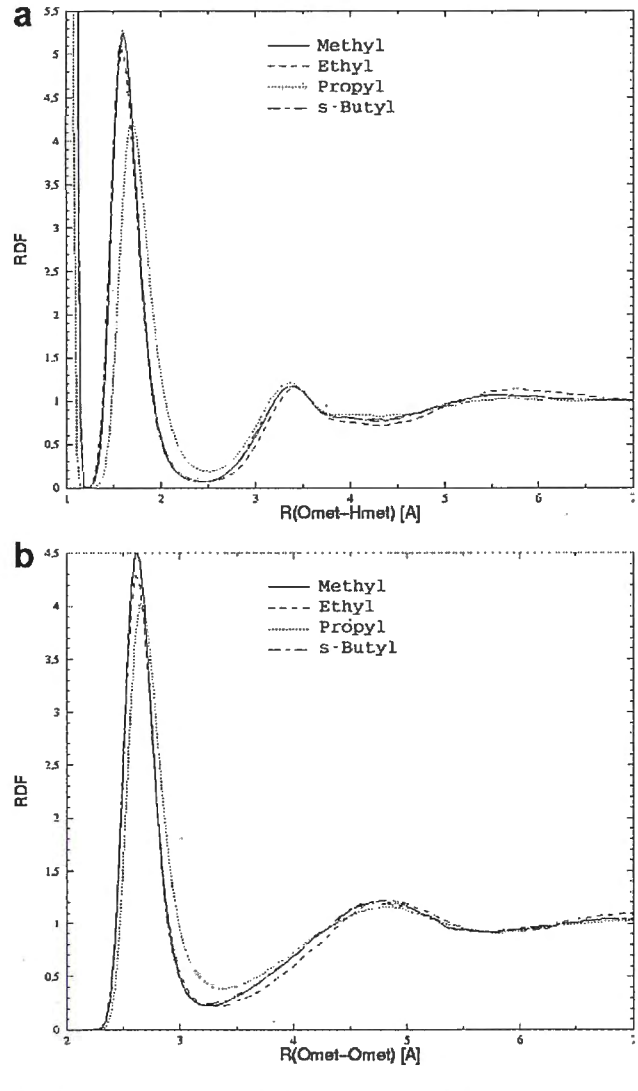

Fig. 5. Comparison of the radial distribution functions between the solvent atoms: **a** Omet–Hmet, **b** Omet–Omet for methanol solutions of 2-(*N*,*N*-dialkylaminomethyl)-3,4,6-trichlorophenols. The first peak at the radial distribution function Omet–Hmet was cut because it is related to the hydrogen atoms from the OH groups

temperature, and therefore producing a more organized solvent structure, increases the concentration of the zwitterionic form. Additionally, the negative experimental value of the entropy change upon the intramolecular proton-transfer process indicates that there should be some changes in the solvent structure towards more organized systems, at least locally. The present study does not address the question of the reaction pathway of the intramolecular proton-transfer process, meaning that we did not study the energy barrier of this process and the significance of the proton tunneling. Therefore, we plan to investigate this further in computational studies that include application of quantum dynamics methods.

Acknowledgements. This work was supported by KBN grant no. 3T09A 041 15. The authors are thankful to Jerzy Janski from the University of Wroclaw for his help in computer simulations and to Lingyi Zheng from the Department of Statistics, West Virginia University, and to Vladimir Hnizdo and James Snyder from the National Institute for Occupational Safety and Health for their help in the preparation of this document.

References

1. Koll A, Wolschann P (1999) Monatssch Chem 130: 983
2. Koll A, Wolschann P (1996) Monatssch Chem 127: 475
3. Fedorowicz A, Mavri J, Bala P, Koll A Chem Phys Lett 289: 457
4. Fedorowicz A, Koll A (2000) J Mol Liq 87: 1
5. Benno R (1959) Die Mannich Reaction. Springer, Berlin Heidelberg New York
6. Zundel G, Fritsch J (1984) J Phys Chem 88: 6295
7. Rospenk M (1990) J Mol Struct 221: 109

8. Rospenk M, Ruminskaya IG, Schreiber VM (1982) Zh Prikl Spectr 36: 756
9. Press WH, Teukolsky SA, Vetterling WT, Flannery BP (1995) Numerical recipes in FORTRAN. The art of scientific computing, 2nd edn. Cambridge University Press, Cambridge
10. Becke AD (1993) J Chem Phys 98: 5648
11. Lee C, Yang W, Parr RG (1988) Phys Rev B 37: 785
12. Frisch MJ, Trucks GW, Schlegel HB, Gill PMW, Johnson BG, Robb MA, Cheeseman JR, Keith T, Petersson GA, Montgomery JA, Raghavachari K, Al-Laham MA, Zakrzewski VG, Ortiz JV, Foresman JB, Cioslowski P, Stefanov BB, Nanayakkara A, Andres JL, Replogle ES, Gomperts R, Martin RL, Fox DJ, Binkley JS, Defrees DJ, Baker J, Stewart JP, Head-Gordon M, Gonzalez C, Pople JA (1998) Gaussian98, revision A.7. Gaussian, Pittsburgh, PA
13. Miertus S, Tomasi J (1982) Chem Phys 65: 239
14. Tomasi J, Persico M (1994) Chem Rev 94: 2027
15. Besler BH, Merz Jr KM, Kollman PA (1990) J Comput Chem 11: 431
16. Singh UC, Kollman PA (1984) J Comput Chem 5: 129
17. van Gunsteren WF, Billeter SR, Eising AA, Hunerberger PH, Kuger P, Mark AE, Scott WRP, Tironi IG (1996) Biomolecular simulations: The GROMOS96 manual and user guide. Biomos, Zurich
18. Berendsen HJC, Postma JP, van Gunsteren WF, DiNola A, Haak JR (1984) J Chem Phys 81: 3684
19. Allen MP, Tildesley DJ (1987) Computer simulations of liquids. Clarendon, Oxford
20. Tuckerman ME, Marx D (2001) Phys Rev Lett 86: 4946